We are IntechOpen,
the world's leading publisher of Open Access books
Built by scientists, for scientists

6,900
Open access books available

185,000
International authors and editors

200M
Downloads

154
Countries delivered to

Our authors are among the

TOP 1%
most cited scientists

12.2%
Contributors from top 500 universities

BOOK CITATION INDEX
CLARIVATE ANALYTICS
INDEXED

WEB OF SCIENCE™

Selection of our books indexed in the Book Citation Index
in Web of Science™ Core Collection (BKCI)

Interested in publishing with us?
Contact book.department@intechopen.com

A Model for Dynamic Optimization of Pitch-Regulated Wind Turbines with Application

Karam Y. Maalawi

Additional information is available at the end of the chapter

1. Introduction

With the growing demand for cost-effective wind energy, optimization of wind turbine components has been gaining increasing attention for its acknowledged contributions made to design enhancement, especially in early stages of product development. One of the major design goals is the accurate determination of structural dynamics and control, which is directly related to fatigue life and cost of energy production: a major design goal in exploiting wind energy. Modern wind turbines are designed with pitch-regulated rotor blades, which have to be able to turn around their longitudinal axis several times per second in order to face the rapidly changing wind direction. This fact emphasizes the need to improve the design of pitch mechanisms using optimization techniques in order to increase availability of the turbines and reduce their maintenance overheads. (Florin et al., 2004; Jason et al. 2005) demonstrated the different tools for performing the analysis of the interaction between the mechanical system of the wind turbine and the electrical grid as well as the calculation of the dynamic loads on the turbine structure. In case of stronger winds it is necessary to waste part of the excess energy of the wind in order to avoid damaging the wind turbine. All wind turbines are therefore designed with some sort of power control. There are different ways of doing this safely on modern wind turbines: pitch, active stall and passive stall controlled wind turbines.

On a pitch controlled wind turbine (Hansen et al., 2005) the turbine's electronic controller checks the power output of the turbine several times per second. When the power output becomes too high, it sends an order to the blade pitch mechanism which immediately pitches (turns) the rotor blades slightly out of the wind. Conversely, the blades are turned back into the wind whenever the wind drops again. The rotor blades thus have to be able to turn around their longitudinal axis (to pitch) as shown in Fig. 1. The pitch mechanism

is usually operated using hydraulics or electric stepper motors. Fig. 2 shows the optimal operational conditions of a pitch-controlled 2 MW wind turbine. During normal operation the blades will pitch a fraction of a degree at a time, and the rotor will be turning at the same time. The computer will generally pitch the blades a few degrees every time the wind changes in order to keep the rotor blades at the optimum angle to maximize output power for all wind speeds.
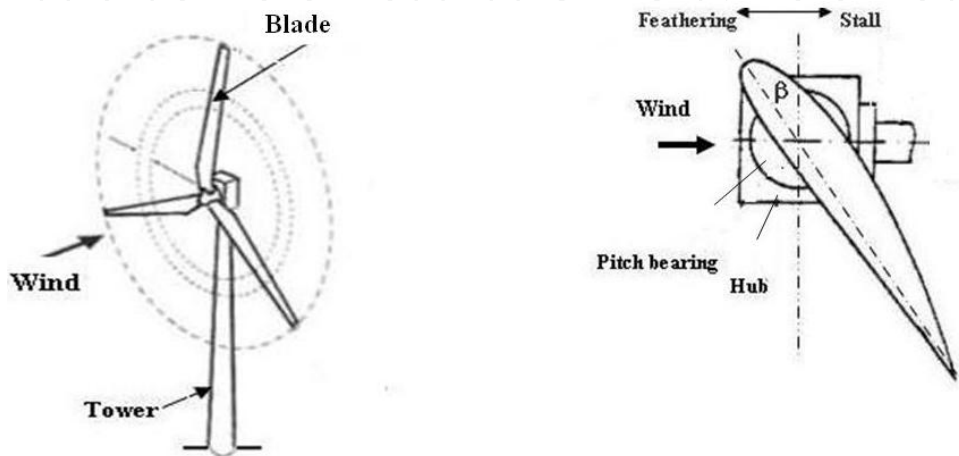

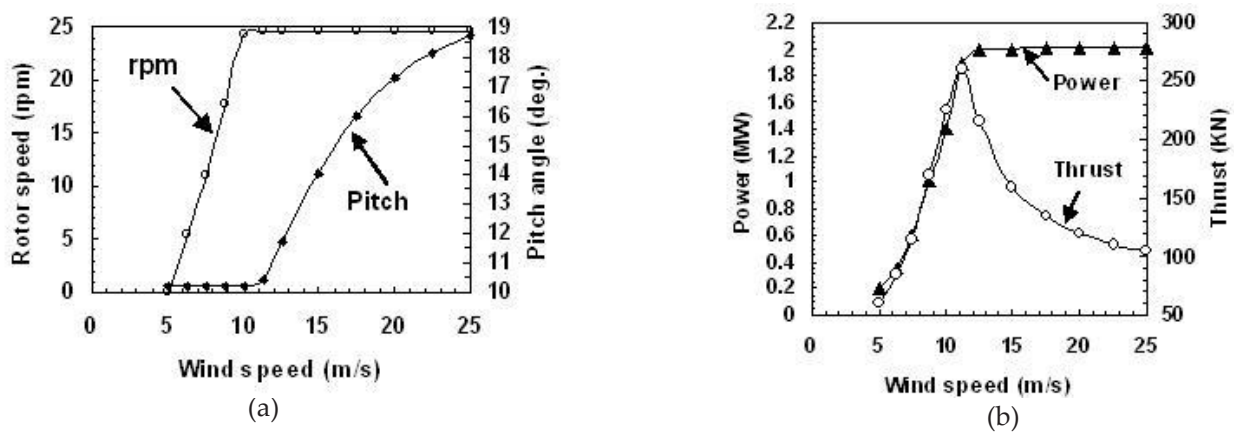**Figure 1.** Limiting power output using pitch control.

Figure 2. Operational conditions of a pitch-controlled, 2.0 MW wind turbine (Hansen et al., 2005)

On the other hand, passive stall controlled wind turbines (Leithed & Conner, 2002; Hoffmann, 2002) have the rotor blades bolted onto the hub at a fixed angle. The geometry of the rotor blade profile however has been aerodynamically designed to ensure that

the moment the wind speed becomes too high; it creates turbulence on the side of the rotor blade which is not facing the wind. This stall prevents the lifting force of the rotor blade from acting on the rotor. The rotor blade of a stall controlled wind turbine is twisted slightly along its longitudinal axis. This is partly done in order to ensure that the rotor blade stalls gradually rather than abruptly when the wind speed reaches its critical value. The basic advantage of stall control is that one avoids moving parts in the rotor itself, and a complex control system. On the other hand, stall control represents a very complex aerodynamic design problem, and related design challenges in the structural dynamics of the whole wind turbine, e.g. to avoid stall-induced vibrations. Around two thirds of the wind turbines currently being installed in the world are stall controlled machines.

Larger wind turbines (1-MW and up) are being developed with an active stall power control mechanism (Hoffmann, 2002). Technically the active stall machines resemble pitch controlled machines, since they have pitchable blades. In order to get a reasonably large torque at low wind speeds, the machines will usually be programmed to pitch their blades much like a pitch controlled machine at low wind speeds. One of the advantages of active stall is that one can control the power output more accurately than with passive stall, so as to avoid overshooting the rated power of the machine at the beginning of a gust of wind. Another advantage is that the machine can be run almost exactly at rated power at all high wind speeds. A normal passive stall controlled wind turbine will usually have a drop in the electrical power output for higher wind speeds, as the rotor blades go into deeper stall. As with pitch control it is largely an economic question whether it is worthwhile to pay for the added complexity of the machine, when the blade pitch mechanism is added. One of the most cost-effective solutions in reducing the produced vibrations and avoiding pitch-control failures on wind turbines (see Fig.3) is to separate the natural frequencies of the blade structure from the critical exciting pitching frequencies (Bindner et al., 1997). This would avoid resonance where large amplitudes of torsional vibration could severely damage the whole structure. The frequency-placement technique (Pritchard & Adelman, 1990; Maalawi, 2007; Maalawi & Badr, 2010) is based on minimizing an objective function constructed from a weighted sum of the squares of the differences between each important frequency and its desired (target) value. Approximate values of the target frequencies are usually chosen to be within close ranges; sometimes called frequency-windows; of those corresponding to a reference baseline design, which are adjusted to be far away from the critical exciting frequencies. Direct maximization of the system natural frequencies (Shin et al., 1988; Maalawi & EL-Chazly, 2002) is also favorable for increasing the overall stiffness-to-mass ratio level of the blade structure being excited. This may further other design objectives such as higher stability and fatigue life and lower cost and noise levels. (Maalawi & Negm 2002) considered the optimal frequency design of a wind turbine blade in flapping motion. They used an exact power series solution to determine the exact mode shapes and the aeroelastic stability boundaries, where conspicuous design trends were given for optimum blade configurations. Both primal and dual optimization problems were thoroughly examined.

Figure 3. Typical blade failure of a three-bladed, 2 MW wind turbine

The scope of this chapter is not just to apply optimization techniques and find an optimum solution for the problem under study. The main aim, however, is to first; perform the necessary exact dynamical analysis of a pitch-regulated wind turbine blade by solving the exact governing differential equation using analytical Bessel's functions. Secondly, the behavior of the pitching fundamental frequency augmented with the mass equality constraint will be investigated in detail to see how it changes with the selected design variables. The associated optimization problem is formulated by considering two forms of the objective function. The first one is represented by a direct maximization of the fundamental frequency, while the second considers minimization of the square of the difference between the fundamental frequency and its target or desired value. In both strategies, an equality constraint is imposed on the total structural mass in order not to violate other economic and performance requirements. Design variables encompass the tapering ratio, blade chord and skin thickness distributions, which are expressed in dimensionless form, making the formulation valid for a variety of blade configurations. The torsional stiffness simulating the flexibility of the inboard panel near the rotor hub is also included in the whole set of design variables. Case studies include the locked and unlocked conditions of the pitching mechanism, in which the functional behavior of the frequency has been thoroughly examined. The developed exact mathematical model guarantees full separation of the frequency from the undesired range which resonates with the pitching frequencies. In fact, the mathematical procedure implemented, combined with exact Bessel's function solutions, can be beneficial tool, against which the efficiency of approximate methods, such as finite elements, may be judged. Finally, it is demonstrated that global optimality can be

achieved from the proposed model and an accurate method for the exact placement of the system natural frequencies has been deduced.

2. Structural dynamic analysis

The isolated blade structure to be analyzed herein is illustrated in figure 4. The inboard panel having ignored length relative to the outboard one is considered as a flexible segment modeled by an equivalent torsion spring. The blade has a polar moment of area I spinning about its longitudinal axis, x, at an angular displacement $B(x,t)$ relative to the pitch bearing at the rotor hub. The blade is analyzed considering the state of free torsional vibration about its elastic axis. The pitching mechanism and the short segment near the hub are assumed to have a linear torsional spring with stiffness K_s. Applying the classical theory of torsion (Rao, 1994), the governing equation of the motion is cast in the following:

$$\frac{\partial}{\partial x}[GJ(x)\frac{\partial B(x,\,t)}{\partial x}]=\rho I(x)\frac{\partial^2 B(x,\,t)}{\partial t^2} \tag{1}$$

which must be satisfied over the interval $0<x<L$.

The associated boundary conditions are described as follows:

Case (I): Pitch is active

$$\text{at blade root (x=0)} GJ\frac{\partial B}{\partial x}\bigg|_{x=0} = 0 \qquad a$$

$$\text{at blade tip (x=L)} GJ\frac{\partial B}{\partial x}\bigg|_{x=L} = 0. \qquad b \tag{2}$$

Case (II): Pitch is inactive

$$\text{at blade root (x=0)} GJ\frac{\partial B}{\partial x}\bigg|_{x=0} = K_s B(0,\,t) \qquad a$$

$$\text{at blade tip (x=L)}|_{x=L} = 0 \qquad b \tag{3}$$

where $GJ(x)$ and $\rho I(x)$ represent the torsional stiffness and the mass polar moment of inertia per unit length, respectively. The twisting angle $B(x,t)$ is assumed to be separable in space and time, $B(x,\,t)=\beta(x).q(t)$, where the time dependence $q(t)$ is harmonic with circular frequency ω. Substituting for $\frac{d^2 q}{dt^2}=-\omega^2 q$, the associated eigenvalue problem can be written directly in the form

$$\frac{d}{dx}[GJ(x)\frac{d\beta}{dx}] + \rho I(x)\omega^2\beta(x)=0 \tag{4}$$
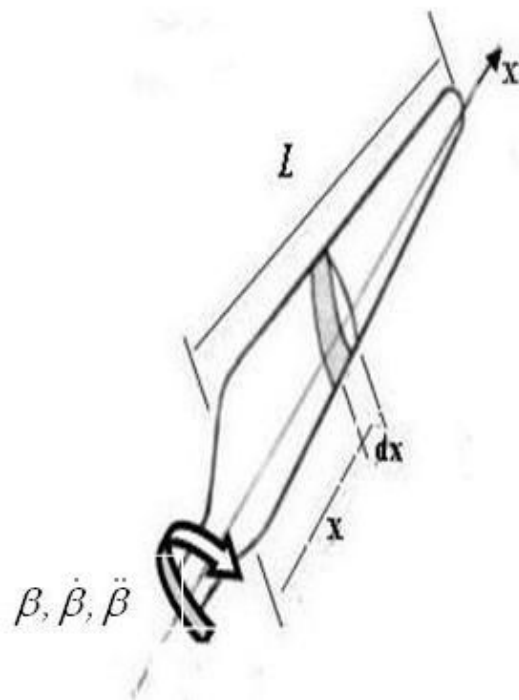
Figure 4. Isolated blade in pitching motion.

The boundary conditions can be obtained from Eqs. (2) and (3). Considering a tapered blade with thin-walled airfoil section (refer to Figures1 & 4), the torsional constant and the second polar moment of area are directly proportional to h and C^3, which are assumed to have the same linear distribution described by the expressions:

$$
\begin{aligned}
C &= C_o(1 - \alpha \hat{x}) \qquad \text{a} \\
h &= h_o(1 - \alpha \hat{x}) \qquad \text{b}
\end{aligned}
\tag{5}
$$

$\hat{x}$ and α are dimensionless parameters defined as:

$$
\hat{x} = \frac{x}{L}, \ \alpha = (1 - \Delta), \ \Delta = C_t \big/ C_0
\tag{6}
$$

where Δ is the taper ratio of the wind turbine blade.

3. Solution procedures

For thin-walled, cellular blade construction, the total structural mass M, the torsional constant $J(x)$, and the polar moment of area $I(x)$ can be determined from the expressions:

$$M = f_1 \int_0^L Ch(x)dx \qquad \text{a}$$

$$J(x) = f_2 C^3 h(x) \qquad \text{b} \qquad\qquad (7)$$

$$I(x) = f_3 C^3 h(x) \qquad \text{c}$$

where f_1, f_2 and f_3 are shape factors depend upon the shape of the airfoil section, number of interior cells and the ratios between the shear web thicknesses and the main wall thickness $h(x)$. It is convenient first to normalize all variables and parameters with respect to a reference design having uniform stiffness and mass distributions with the same material properties, airfoil section, and type of construction as well (see Table 1). The dimensionless expressions for the total mass, torsional constant and polar moment of area are, respectively, given by:

$$\text{Mass} \qquad \hat{M} = \int_0^1 \hat{C}\hat{h}\,d\hat{x} \qquad \text{a}$$

$$\text{Torsion constant} \qquad \hat{J} = \hat{C}^3\hat{h} \qquad \text{b} \qquad\qquad (8)$$

$$\text{Polar moment of area} \quad \hat{I} = \hat{C}^3\hat{h} \qquad \text{c}$$

Therefore, dividing by the corresponding reference design parameters, the governing differential equation takes the following dimensionless form:

$$\beta'' - \frac{4\alpha}{(1-\alpha\hat{x})}\beta' + \hat{\omega}^2\beta = 0; \quad 0 \le \le 1 \qquad\qquad (9)$$

Quantity	Notation	Dimensionless expression
Circular frequency	ω	$\hat{\omega} = \omega L \sqrt{\rho I_r / G J_r}$
Spatial coordinate	x	$\hat{x} = x/L$
Airfoil chord	C	$\hat{C} = C / C_r$
Shear wall thickness	h	$\hat{h} = h / h_r$
Structural mass	M	$\hat{M} = M / M_r$
Torsion constant	J	$\hat{J} = J / J_r \; (= \hat{C}^3\hat{h})$
Polar moment of area.	I	$\hat{I} = I / I_r \; (= \hat{C}^3\hat{h})$
Stiffness coefficient at root	K_s	$\hat{K}_s = \dfrac{K_s}{(G J_r / L)}$

Reference parameters: M_r=structural mass, J_r= torsion constant, I_r=2nd polar moment of area, where C_r=Chord length, h_r=wall thickness, blade taper Δ=1.

Table 1. Definition of dimensionless quantities

The boundary conditions to be satisfied are $\beta' = 0$ at both blade root and tip for the unlocked pitching condition and $\beta' = (\dfrac{\hat{K}_s}{\hat{J}_0})\beta$ at root, $\beta' = 0$ at tip for the locked condition, where the prime denotes here differentiation with respect to $\hat{x}$. Using the transformation $\hat{x} = \dfrac{1}{\alpha} - \dfrac{1}{\hat{\omega}}y$ ($\alpha \neq 0$), Eq. (9) takes the form:

$$\frac{d^2\beta}{dy^2} + \frac{4}{y}\frac{d\beta}{dy} + \beta = 0; \quad \delta \leq y \leq \gamma \tag{10}$$

which can be further transformed to the standard form of Bessel's equation by setting $\beta = \psi / \sqrt{y^3}$, to get

$$y^2\frac{d^2\psi}{dy^2} + y\frac{d\psi}{dy} + (y^2 - \frac{9}{4})\psi = 0 \tag{11}$$

This has the solution

$$\psi(y) = C_1 J_{3/2} + C_2 J_{-3/2} \tag{12}$$

where C_1 and C_2 are constants of integration and $J_{3/2}$ and $J_{-3/2}$ are Bessel's functions of order $k = \pm 3/2$, given by (Edwards & Penney, 2004):

$$J_{3/2}(y) = \sqrt{\frac{2}{\pi y^3}}(\sin y - y\cos y) \qquad \text{a} \tag{13}$$

$$J_{-3/2}(y) = -\sqrt{\frac{2}{\pi y^3}}(\cos y + y\sin y) \qquad \text{b}$$

The exact analytical solution of the associated eigenvalue problem is:

$$\beta(y) = A\left[\frac{y\cos y - \sin y}{y^3}\right] + B\left[\frac{y\sin y + \cos y}{y^3}\right] \tag{14}$$

where A and B are constants depend on the imposed boundary conditions. Applying the boundary conditions, given in Eqs. (2) and (3), and considering only nontrivial solution the frequency equation can be directly obtained. The final derived exact frequency equations for both active and inactive pitching motion in appropriate compacted closed forms are summarized in the following:

$$\text{Baseline design with rectangular planform} \quad (D=1) \quad \hat{\omega}\tan\hat{\omega} = \hat{K}_s / (\hat{h}_o \hat{C}_o^3) \tag{15}$$

$$\text{Active pitching} \quad \tan\hat{\omega} = \frac{3\hat{\omega}(3 + \gamma\delta)}{(\gamma\delta)^2 - 3\gamma^2(1 + \Delta^2) + 9(1 + \gamma\delta)} \tag{16}$$

$$\text{Locked pitching mechanism} \quad \tan\hat{\omega} = \frac{(1 - 3\theta)(3\hat{\omega} - \gamma\delta^2) - 3\gamma^2\delta\theta}{3\gamma\delta(1 - 3\theta) + (3 - \delta^2)(1 - 3\theta + \theta\gamma^2)} \tag{17}$$

The definition of the various quantities in Eqs. (15), (16) and (17) is given in Table (1) and the appendix of nomenclature.

4. Optimization problem formulation

Attractive goals of designing efficient structures of wind generators include minimization of structural weight, maximization of the fundamental frequencies (Maalawi & EL-Chazly, 2002; Maalawi & Negm, 2002; Maalawi & Badr, 2010), minimization of total cost per energy produced, and maximization of output power (Maalawi & Badr, 2003). Another important consideration is the reduction or control of the vibration level. Vibration can greatly influence the commercial acceptance of a wind turbine because of its adverse effects on performance, cost, stability, fatigue life and noise. The reduction of vibration can be attained either by a direct maximization of the natural frequencies or by separating the natural frequencies of the blade structure from the harmonics of the exciting torque applied from the pitching mechanism at the hub. This would avoid resonance and large amplitudes of vibration, which may cause severe damage of the blade. Direct maximization of the natural frequencies can ensure a simultaneous balanced improvement in both of the overall stiffness level and the total structural mass. The mass and stiffness distributions are to be tailored in such a way to maximize the overall stiffness/mass ratio of the vibrating blade. The associated optimization problems are usually cast in nonlinear mathematical programming form (Vanderplaats, 1999). The objective is to minimize a function $F(\underline{X})$ of a vector $\underline{X}$ of design variables, subject to certain number of constraints $G_j(\underline{X}) \leq 0$, $j=1,2,\ldots m$.

In the present optimization problem, two alternatives of the objective function form are implemented and examined. The first one is represented by a direct maximization of the fundamental frequency, which is expressed mathematically as follows:

$$\text{Maximize} \quad F(\underline{X}) = -\hat{\omega}_1 \tag{18}$$

where $\hat{\omega}_1$ is the normalized fundamental frequency (see Table1) and $\underline{X} = (\hat{C}_o, \hat{h}_o, \Delta)$ is the chosen design variable vector. The second alternative is to minimize the square of the difference between the fundamental frequency $\hat{\omega}_1$ and its target or desired value $\hat{\omega}^*$, i.e.

$$\text{Minimize} \quad F(\underline{X}) = \left(\hat{\omega} - \hat{\omega}^*\right)^2 \tag{19}$$

Both objectives are subject to the constraints:

$$\text{Mass constraint:} \quad \hat{M} = \int_0^1 \hat{C}\, \hat{h}\, d\hat{x} = 1 \tag{20}$$

$$\text{Side constraints}: \underline{X}_L \leq \underline{X} \leq \underline{X}_u \tag{21}$$

where $\underline{X}_L$ and $\underline{X}_U$ are the lower and upper limiting values imposed on the design variables vector $\underline{X}$ in order not to obtain unrealistic odd-shaped designs in the final optimum solutions. Approximate values of the target frequencies are usually chosen to be within close ranges; sometimes called frequency – windows; of those corresponding to an initial baseline design, which are adjusted to be far away from the critical exciting pitching frequencies. Several computer program packages are available now for solving the above design optimization model, which can be coded to interact with structural and eigenvalue analyses software. Extensive computer implementation of the models described by Eqs. (18-21) have revealed the fact that maximization of the fundamental frequency is a much better design criterion. If it happened that the maximum frequency violates frequency windows, which was found to be a rare situation, another value of the frequency can be chosen near the global optima, and the frequency equations (15-17) can be solved for any one of the unknown design variables instead. Considering the frequency-placement criterion, it was found that convergence towards the optimum solution, which is also too sensitive to the selected target frequency, is very slow.

5. Optimization techniques

The above optimization problem described by Eqs.(18-21) may be thought of as a search in an 3-dimensional space for a point corresponding to the minimum value of the objective function and such that it lie within the region bounded by the subspaces representing the constraint functions. Iterative techniques are usually used for solving such optimization problems in which a series of directed design changes (moves) are made between successive points in the design space. The new design $\underline{X}_{i+1}$ is obtained from the old one $\underline{X}_i$ as follows:

$$\underline{X}_{i+1} = \underline{X}_i + a_i \underline{S}_i \tag{22}$$

$$\text{Such that } F(X_{i+1}) < F(X_i) \tag{23}$$

where the vector $\underline{S}_i$ defines the direction of the move and the scalar quantity α_i gives the step length such that $\underline{X}_{i+1}$ does not violate the imposed constraints, $G_j(X)$. Several optimization techniques are classified according to the way of selecting the search direction $\underline{S}_i$. In general, there are two distinct formulations (Vanderplaats, 1999): the constrained formulation and the unconstrained formulation. In the former, the constraints are considered as a limiting

subspace. The method of feasible directions is one of the most powerful methods in this category. In the unconstrained formulation, the constraints are taken into account indirectly by transforming the original problem into a series of unconstrained problems. A method, which has a wide applicability in engineering applications, is the penalty function method.

The *MATLAB* optimization toolbox is a powerful tool that includes many routines for different types of optimization encompassing both unconstrained and constrained minimization algorithms (Vekataraman, 2009). One of its useful routines is named *"fmincon"* which implements the method of feasible directions in finding the constrained minimum of an objective function of several variables starting at an initial design. The search direction $\underline{S}_j$ must satisfy the two conditions $\underline{S}_j . \nabla F < 0$ and $\underline{S}_j . \underline{\nabla} G_j < 0$, where $\underline{\nabla} F$ and $\underline{\nabla} G_j$ are the gradient vectors of the objective and constraint functions, respectively. For checking the constrained minima, the Kuhn-Tucker test (Vanderplaats, 1999) is applied at the design point $\underline{X}_D$, which lies on one or more set of active constraints. The Kuhn-Tucker equations are necessary conditions for optimality for a constrained optimization problem and their solution forms the basis to the method of feasible directions.

6. Results and discussions

The developed mathematical model has been implemented for the proper placement of the frequencies of typical blade structure in free pitching motion. Optimum solutions are obtained by invoking the *MATLAB* routine *"fmincon"* which interacts with the eigenvalue calculation routines. The target frequencies, at which the pitching frequencies needed to be close to, depend on the specific configuration and operating conditions of the wind machine. Various cases of study are examined including, blades with both locked and unlocked pitching conditions. The main features and trends in each case are presented and discussed in the following sections.

6.1. Unlocked pitching mechanism condition

Considering first the case of active pitching, figure 5 shows the variation of the first three resonant frequencies with the tapering ratio. It is seen that the frequencies decrease with increasing taper. Blades having complete triangular planforms shall have the maximum frequencies which is favorable from structural design point of view. However, such configurations violate the requirement of having an efficient aerodynamic surface producing the needed mechanical power. Now, in order to place any frequency at its desired value $\hat{\omega}_i^*$, i=1,2,3, the first step is to calculate the dimensionless frequency $\hat{\omega}_i$, i=1,2,3, for known properties of the blade material and airfoil section, and then obtain the corresponding value of the taper ratio from the curves presented in figure 5. The next step is to choose appropriate value for the dimensionless thickness $\hat{h}_o$ at the blade root and find the corresponding chord length $\hat{C}_o$ at the determined taper ratio (see figure 6), which should satisfy the equality mass constraint expressed by Eq. (20). It is to be noticed here that the dimensionless wall thickness $\hat{h}_o$ at root shall be constrained to be greater than a preassigned lower bound,

which can either be determined from the minimum available sheet thicknesses or from considerations of wall instability that might happen by local buckling.
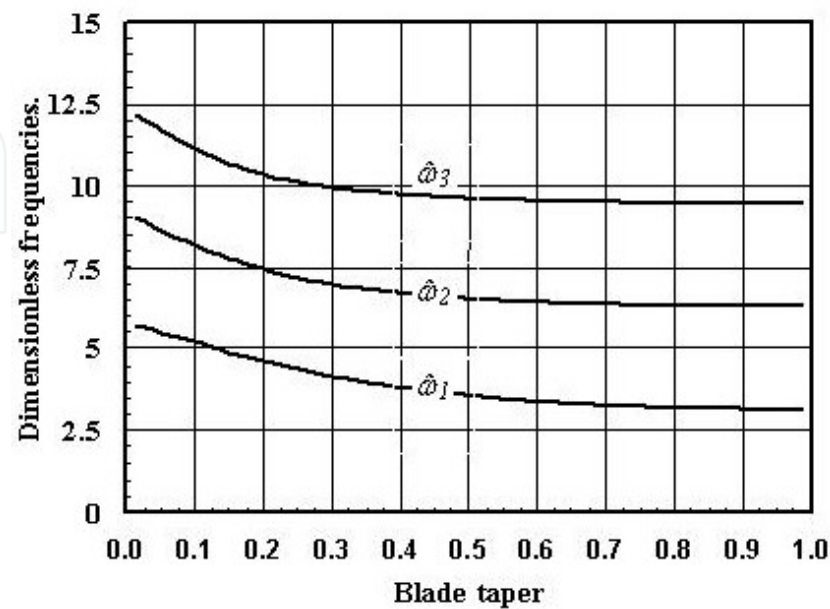

Figure 5. Normalized frequencies of free pitching motion (Unlocked blade)
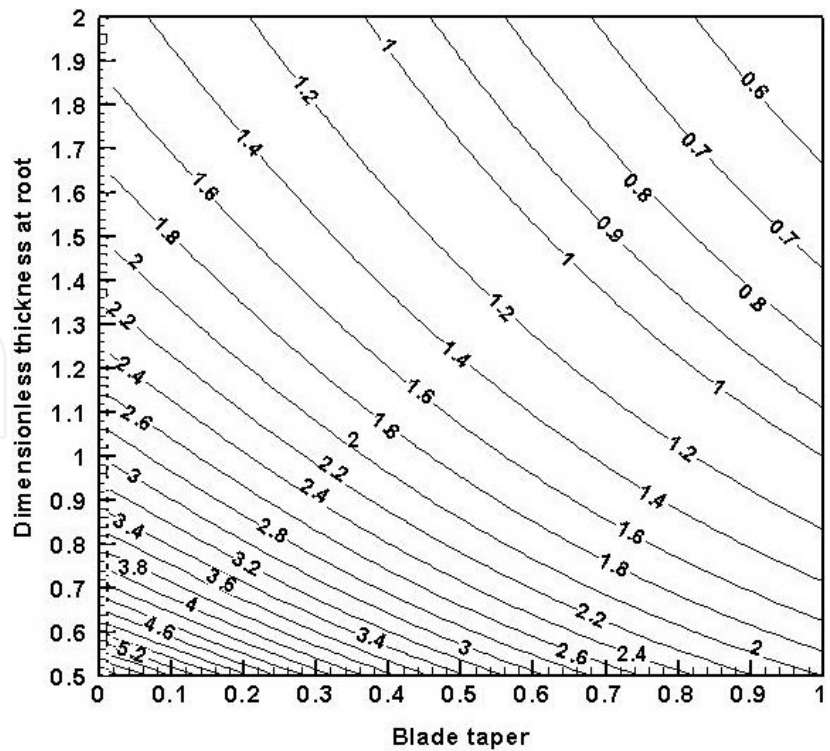

Figure 6. Optimized tapered blades with constant mass ($\hat{C}_o$ - Level curves, $\hat{M}$ =1)

6.2. Condition of locked pitching mechanism

Extensive computer solutions for the frequency equation (17) have indicated the existence of the frequency level curves in the selected design space. Figures 7, 8 and 9 depicts, respectively, the developed frequency charts for the design cases of locked pitching mechanism with $\hat{K}_s$ = 10, 100 and 1000 representing flexible, semi-rigid and rigid blade root. Any other specific case can be easily obtained by following and applying the same procedures outlined before in sections 3 and 4. It is seen from the figures that the frequency function is well behaved and continuous in the selected design space (h_o, C_o). Actually, these charts represent the fundamental pitching frequency augmented with the equality mass constraint. Therefore, they reveal very clearly how one can place the frequency at its target value without the penalty of increasing the total mass of the main blade structure. Such charts also can be utilized if one is seeking to maximize the frequency under equality mass constraint. Maximization of the natural frequencies has the benefit of improving the overall stiffness/mass ratio of the vibrating structure (Maalawi and Negm, 2002).
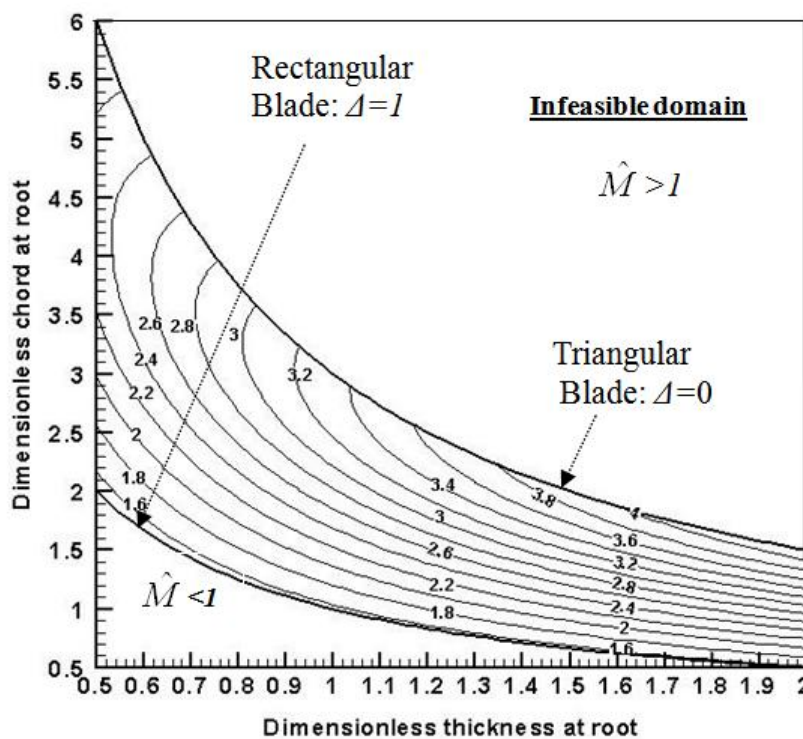

Figure 7. Augmented frequency-mass contours ($\hat{\omega}_1$) for a blade with flexible blade root: $\hat{K}_s$ = 10 ($\hat{M}$ =1)

As seen, the developed contours depicted in figure 7 has a banana- shaped profile bounded by two curved lines; the one from above represents a triangular blade ($\Delta=0$) and the other

lower one represents a rectangular blade geometry ($\Delta=1$). It is not allowed to penetrate these two borderlines in order not to violate the imposed mass equality constraints. Each point inside the feasible domain in the middle corresponds to different mass and stiffness distributions along the blade span, but the total structural mass is preserved at a constant value equals to that of the rectangular reference blade. The lower and upper empty regions represent, respectively, infeasible blade designs with structural mass less or greater than that of the baseline design. The global optimal design is too close to the design point $\{\hat{C}_o, \hat{h}_o, \Delta\}=\{1.202, 2.011, 0.207\}$ with $\hat{\omega}_{1,max}=2.6472$. If it happened that such global optima violates frequency windows, another value of the frequency can be taken near the optimum point, and an inverse approach is utilized by solving the frequency equation for any one of the unknown design variables instead.
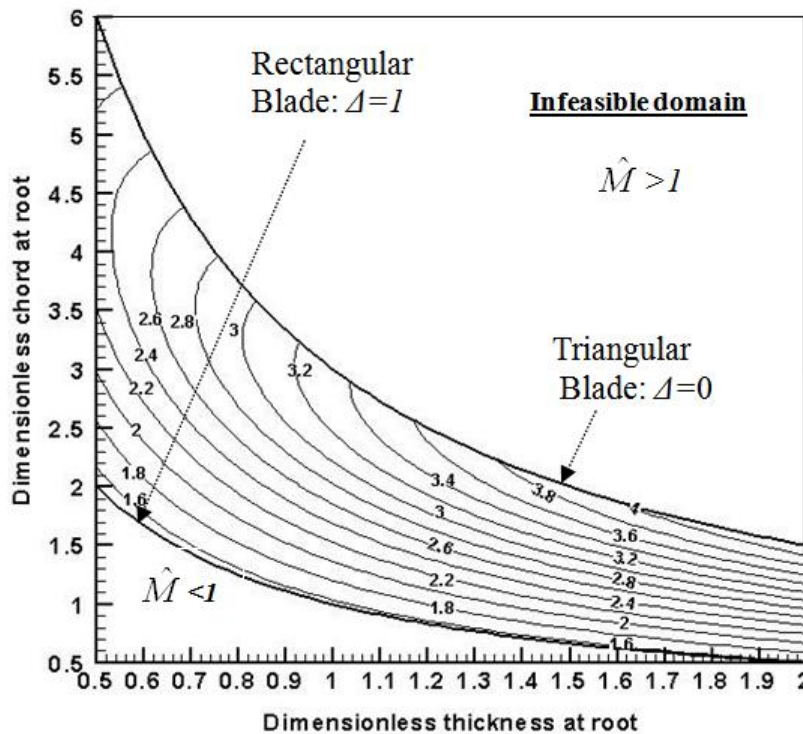

Figure 8. Level curves of $\hat{\omega}_1$ for a semi-rigid blade root; $\hat{K}_s=100$, $\hat{M}=1$.

Other cases for semi-rigid and rigid blade root are shown in figures 8 and 9. It is seen that the contour lines become more flatten and parallel to the two borderlines as the hub stiffness increases. The calculated maximum values of the fundamental pitching frequency are 4.2161 at the design point $\{1.5, 2, 0\}$ for $\hat{K}_s=100$ and 4.4825 at the same design point for $\hat{K}_s=1000$. Such optimal blade designs having triangular planform are

favorable from structural point of view. However, such configurations violate the re‐ quirement of having an efficient aerodynamic surface producing the needed mechanical power. In all, it becomes now possible to choose the desired maximum frequency, which is far away from the excitation frequencies, and obtain the corresponding opti‐ mum variables directly from the developed frequency charts. Actually, the charts repre‐ sent the fundamental frequency function augmented with the imposed mass equality constraint so that the problem may be treated as if it were an unconstrained optimiza‐ tion problem. Table 2 summarizes the final optimum solutions showing that good blade patterns ought to have the lowest possible tapering ratio. This means that the optimum design point is always very close to the lower limiting value imposed on the blade ta‐ pering ratio, i.e. 0.25.
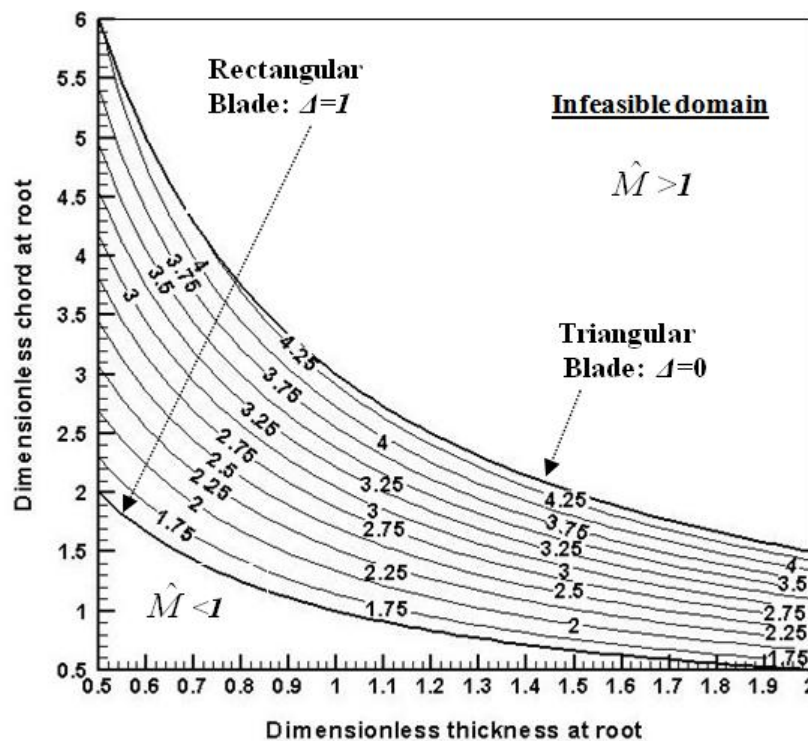

Figure 9. Level curves of $\hat{\omega}_1$ for a rigid blade root; $\hat{K}_s=1000$, $\hat{M}=1$.

Figure 10 depicts the variation of the maximum fundamental frequency with the stiffness at blade root. It is seen that the frequency decreases sharply with increasing the stiffness coeffi‐ cient up to a value of 10, after which it increases in the interval between $\hat{K}_s=10$ and 100 and then remain approximately constant at the principal values $\pi/2$ and π. The average attained optimization gain reached a value of about 86.95 % as measured from the reference design.
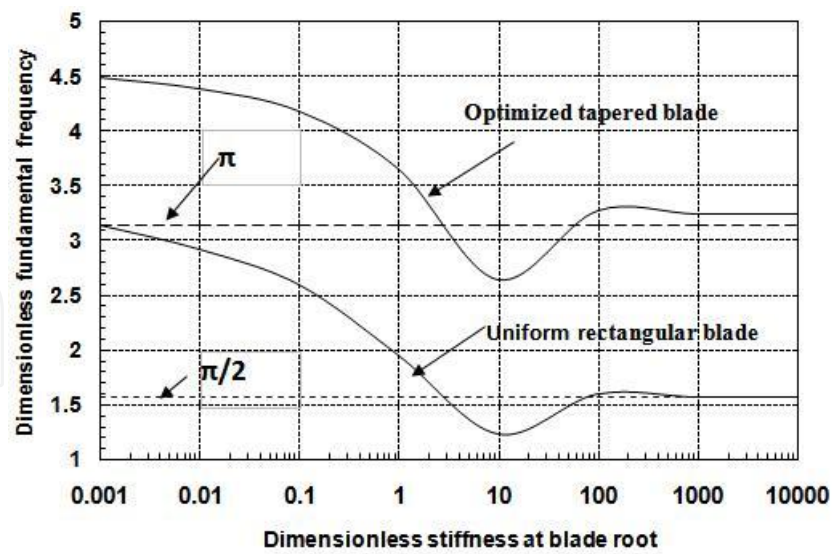
Figure 10. Variation of the constrained maximum fundamental frequency $\hat{\omega}_{1,\max}$ with blade root stiffness $\hat{K}_s$, ($\hat{M}$=1)

Stiffness coefficient ($\hat{K}_s$)	Reference rectangular ($\hat{C}_o, \hat{h}_o, \Delta$)=(1, 1, 1)	Optimized tapered blade	
	$\hat{\omega}_1$	$\hat{\omega}_{1,\max}$	($\hat{C}_o, \hat{h}_o, \Delta$)$_{optimum}$
0.0 (Unlocked pitch)	3.1416 (π)	4.4871	(1.4520, 1.5861, 0.2514)
0.01	2.9235	4.3891	(1.7289, 1.3122, 0.2522)
0.1	2.5987	4.1871	(1.5973, 1.4221, 0.2541)
1	1.9546	3.6542	(1.3794, 1.6583, 0.2527)
10	1.2322	2.6467	(1.1651, 1.9546, 0.2504)
100	1.59811	3.2741	(1.2533, 1.7982, 0.2532)
1000	1.5731	3.2435	(1.4523, 1.5822, 0.2531)
∞ (Perfect rigidity)	1.5708 (π/2)	3.2389	(1.4763, 1.5428, 0.2529)
Equality mass constraint : $\hat{M}$=1 Inequality side constraints: $0.5 \leq \hat{C}_o \leq 2.0$ $0.25 \leq \hat{h}_o \leq 2.0$ $0.25 \leq \Delta \leq 0.75$			

Table 2. Constrained optimal solutions for different blade root flexibility.

6.3. Model validation: Actual operation case

As a part of the ministry of electricity plans for wind energy programs in Egypt, a study is currently performed concerning the design and manufacture of an upwind, two-bladed, pitch-controlled, horizontal-axis wind turbine producing *100 KW* electrical power output. The wind turbine will be erected for testing and experimental investigation in the western coast of the Gulf of Suez near Hurghada, which has the most favorable wind condition with average wind speeds between *7-12 m/s*. The followings are the relevant values of the reference blade design parameters:

- Planform: rectangular *(taper Δ=1)*, chord C_r=*1.0 m*, Elastic length *L=12.5 m*.

- Cross section: *NACA 4415* airfoil, single cell construction.

- Wall thickness h_r=*5.0x10^{-3} m*.

- Torsion constant J_r=*1.536 x 10^{-4} m^4*.

- 2nd moment of area I_r=*7.462 x 10^{-4} m^4*.

- Type of material: E-glass/Epoxy composite.

- Equivalent in-plane shear modulus *G=4.7 GPa*, mass density *ρ=1800 kg/m^3*

- Total structural mass: M_r=*250.0 kg*.

- Dimensionless circular frequency:

$\hat{\omega}_r = \pi$ for unlocked pitch

$= \pi/2$ for locked pitch

∴Dimensional circular frequency ω_r = *58.65* $\hat{\omega}_r$ *rad/sec*. (refer to Table 1).

Frequency in *HZ*: $f_r=\omega_r/2\pi$

=*29.325 HZ* (Unlocked condition)

= *14.6625 HZ* (Locked condition)

- Excitation frequency *f=20.0 HZ*.

The final attained optimal design for the case of active pitch is (see Table 2 and Figure 5):

- The first three frequencies are $f_{i,max}$= *41.8846, 67.802, 95.548 HZ*, which corresponds to the optimal chord and thickness distributions:

$C(\hat{x})$= *1.452 (1-0.7486* $\hat{x}$ *) m*

$h(\hat{x})$= *7.931x10^{-3}(1-0.7486* $\hat{x}$ *) m*, $0 \le \hat{x} \le 1$.

Δ=0.2514.

Other cases with different blade root flexibilities can be obtained using the dimensionless optimal solutions given in Table 2.

7. Conclusions

Efficient model for optimizing frequencies of a wind turbine blade in pitching motion has been presented in this chapter. The mathematical formulation is given with dimensionless quantities so as to make the model valid for a real-world wind turbine blade of any size and configuration. It provides exact solutions to the vibration modes of the blade structure in free pitching motion, against which the efficiency of other numerical methods, such as the finite element method, may be judged. Design variables include the chord length of the air-foil section, shear wall thickness and blade tapering ratio. Useful design charts for either maximizing the natural frequency or placing it at its desired (target) value has been developed for a prescribed total structural mass, and known torsional rigidity near blade root. The fundamental frequency can be shifted sufficiently from the range which resonates with the excitation frequencies. In fact the developed frequency charts given in the paper reveal very clearly how one can place the frequency at its proper value without the penalty of increasing the total structural mass. Each point inside the chart corresponds to different mass and stiffness distribution along the span of constant mass blade structure. The given approach is also implemented to maximize the frequency under equality mass constraint. If it happened that the obtained maximum frequency violates frequency windows, another value of the frequency can be taken near the optimum point, and an inverse approach can be applied by solving the frequency equation for any one of the unknown design variables instead. Other factors under study by the author include the use of material grading concept to enhance the dynamic performance of a wind turbine blade. Exciting frequencies due to the turbulent nature of the wind, especially in large wind turbines with different types of boundary conditions, are also under considerations. Another extension of this work is to optimize the aerodynamic and structural efficiencies of the blade by simultaneously maximizing the power coefficient and minimizing vibration level under mass constraint using a muli-criteria optimization technique.

Appendix

$B(x,t)$ pitch angle about blade elastic axis: $B(x, t) = \beta(x).q(t)$,

C chord length of the airfoil section

C_t chord length at blade tip

C_o chord length at blade root

G shear modulus of blade material

h skin thickness of the blade

h_o skin thickness at blade root

I second polar moment of area

J torsion constant of the blade cross section

K_s torsional stiffness coefficient at blade root

L effective blade length

$q(t)$ time dependence of blade pitch angle.

t time variable

X design variables vector.

x distance along blade span measured from chord at root

$\alpha = (1 - \Delta)$

$\beta(x)$ amplitude of the pitch angle

ω circular frequency of pitching motion

$\hat{\omega}$ normalized frequency

$\gamma \qquad (= \hat{\omega} / \alpha)$

$\delta \qquad (= \gamma \Delta)$

ρ mass density of blade material

Δ blade taper ratio (C_t / C_o)

$\theta \; (= \alpha \hat{h}_o \hat{C}_o^3 / \hat{K}_s)$

Author details

Karam Y. Maalawi

National Research Centre, Mechanical Engineering Department, Cairo, Egypt

References

[1] Bindner, H., Rebsdorf A., and Byberg, W., (1997). Experimental investigation of combined variable speed / variable pitch controlled wind turbines. European Union Wind Energy Conference, EWEC97, Dublin, Ireland.

[2] Edwards, C.H. and Penney, D.E. (2004). Elementary differential equations with applications. Prentice-Hall, Inc., Englewood Cliffs, New Jersey.

[3] Florin Iov, Hansen, A.D., Jauch, C., Sorensen, P., & Blaabjerg F. (2004). Advanced tools for modeling, design and optimization of wind turbine systems. Proceedings of

NORDIC Wind Power Conference, Chalmers University of Technology, Goteborg-Sweden, 1-2 March, 2004.

[4] Hansen, M.H., Hansen, A., Larsen, T.J., Oye, S.I., Sorensen, P., & Fuglsang P. (2005). Control design for a pitch regulated, variable speed wind turbine. Riso National Laboratory, Riso-R-1500 (EN), Roskilde, Denmark.

[5] Hoffmann, R. (2002). *A comparison of control concepts for wind turbines in terms of energy capture*. M.Sc. Thesis, Department of Electronic and Information, University of Darmstadt, Germany.

[6] Jason, M. Jonkman, Marshall L. & Buhl, Jr. (2005). FAST User's Guide. Technical Report, NREL/EL-500-38230.

[7] Leithed, W.E. and Conner, B.C., (2002). Control of variable speed wind turbines: Dynamic modeling. *International Journal of Control*, 73(13), 1173-1188.

[8] Maalawi, K.Y. and Negm, H.M. (2002). Optimal frequency design of wind turbine blades. *Journal of Wind Engineering and Industrial Aerodynamics*, 90(8), 961-986.

[9] Maalawi, K.Y. and El-Chazly, N.M. (2002). Global optimization of multi-element beam-type structures. The Second International Conference on *Advances in Structural Engineering and Mechanics*, ASEM'02, Busan, South Korea, August 21-23.

[10] Maalawi, K.Y. and Badr, M.A. (2003). A practical approach for selecting optimum wind rotors. *International Journal of Renewable Energy*, 28, 803-822.

[11] Maalawi, K.Y. (2007). A model for yawing dynamic optimization of a wind turbine structure. *International Journal of Mechanical Sciences*, 49, 1130-1138.

[12] Maalawi, K.Y. and Badr, M.A. (2010). Frequency optimization of a wind turbine blade in pitching motion. *Journal of Power and Energy*, JPE907, Proc. IMechE Vol. 224, Part A, pp. 545-554.

[13] Rao, J.S. (1994). Advanced theory of vibration, Wiley Eastern Limited, New York.

[14] Pritchard, J.I. and Adelman, H.M. (1990). Optimal placement of tuning masses for vibration reduction in helicopter rotor blades, *AIAA Journal*, 28(2), 309-315.

[15] Shin, Y.S., Haftka, R.T., Plaut, R.H. (1988). Simultaneous analysis and design of eigenvalue maximization, *AIAA Journal*, 26(6), 738-744.

[16] Vanderplaats, G.N. (1999). Numerical optimization techniques for engineering design with applications. McGraw Hill, New York

[17] Vekataraman, P. (2009). Applied optimization with *MATLAB* programming. 2nd Edition, Wiley, New York.